

# Orbital ordering in $\text{LaMnO}_3$ : Electron-electron versus electron-lattice interactions

Wei-Guo Yin,<sup>1</sup> Dmitri Volja,<sup>1,2</sup> and Wei Ku<sup>1,2</sup>

<sup>1</sup>*Physics Department, Brookhaven National Laboratory, Upton, NY 11973*

<sup>2</sup>*Physics Department, State University of New York, Stony Brook, NY 11790*

(Dated: Received May 24, 2019)

The relative importance of electron-lattice (e-l) and electron-electron (e-e) interactions in ordering orbitals in  $\text{LaMnO}_3$  is systematically examined within the LDA+ $U$  approximation of density functional theory. A realistic effective Hamiltonian is derived from novel Wannier functions analysis of the electronic structure. Surprisingly, e-l interaction ( $\simeq 0.9$  eV) alone is found insufficient to stabilize the orbital ordered state. On the other hand, e-e interaction ( $\simeq 1.7$  eV) not only induces orbital ordering, but also greatly facilitates the Jahn-Teller distortion via enhanced localization. Further experimental means to quantify the competition between these two mechanisms are proposed.

PACS numbers: 75.47.Lx, 71.70.-d, 71.70.Ej, 75.30.Fv

Study of perovskite manganites has been one of the main focuses of recent research in condensed matter physics, not only because of their great potentials in technological applications related to colossal magnetoresistance (CMR) in  $\text{La}_{1-x}\text{Ca}_x\text{MnO}_3$ , but also because these strongly correlated compounds are ideally instrumental to the understanding of the complex interplay of the charge, spin, orbital, and lattice degrees of freedom that leads to abundant fascinating phenomena, including long range order in all the above channels [1].

The unusual orbital degree of freedom in the manganites, which is the focus of our study, originates from the singly occupied degenerate  $e_g$  states ( $d_{z^2}$  and  $d_{x^2-y^2}$ ) of the  $\text{Mn}^{3+}$  3d electrons in the high-spin configuration ( $t_{2g}^3 e_g^1$ ), owing to the octahedral crystal-field splitting and strong Hund's coupling. This orbital degeneracy makes the  $\text{Mn}^{3+}$  ion Jahn-Teller (JT) active: the degeneracy can be split via biaxial distortion of the surrounding oxygen octahedron.

Currently, one of the critical questions on the manganites is the interplay of electron-lattice (e-l) and electron-electron (e-e) interactions [2, 3, 4, 5]. Theoretically, although both interactions have similar effects on various aspects [2], they clearly play substantially different roles, for example, in magnetism [3, 5]. However, even for the simplest parent compound,  $\text{LaMnO}_3$  (which presents prototype orbital order (OO) and strongest JT-distortion in the family), various spectral measurements to date [6, 7, 8, 9, 10, 11] have left two possible mechanisms for the OO in dispute: the cooperative JT e-l effect [12] and the e-e superexchange effect [13]. To our knowledge, there is no clear experimental evidence to support one over the other, due to lack of “signatures” in distinguishing these two mechanisms. This leads to great confusions in the field: for example, whether a new type of elementary excitations called orbiton has been observed in Raman scattering spectroscopy [10, 11], and more generally which interaction dominates localization of the  $e_g$  electrons and thus facilitates the CMR effects upon doping  $\text{LaMnO}_3$  [14, 15]. It is thus important and timely to

discern the real roles of e-e and e-l interactions.

In this Letter, the electronic structure of the prototype  $\text{LaMnO}_3$  is systematically analyzed, aiming to quantify the relative importance of e-e and e-l interactions in ordering the orbitals. A realistic effective Hamiltonian for the low energy  $e_g$  states including both interactions is derived from novel Wannier functions (WFs) analysis [7, 16] of results from density functional theory, with the effective e-e interaction  $U_{\text{eff}} \simeq 1.7$  eV, JT splitting  $\Delta_{\text{JT}} \simeq 0.9$  eV, and octahedral-tilting induced tetragonal crystal field  $E_z \simeq 0.12$  eV. Surprisingly, e-l interaction alone is found insufficient to stabilize OO. On the other hand, e-e interaction not only induces OO, but also greatly facilitates the JT distortion by strongly localizing the electrons. The present results provide new insight into OO in  $\text{LaMnO}_3$ , and place stringent constraints on any quantitative theories of excitations and CMR in the manganites. Furthermore, our analysis indicates certain *competition* between different mechanisms, which allows direct experimental determination of their relative strengths.

In this study, a new theoretical scheme is developed for *general* quantitative description of strongly correlated systems. In brief, quantitative tight-binding description is first obtained via low-energy symmetry-specific WFs, based on the electronic structure calculated with the LDA+ $U$  method [17, 18] (that relieves the notorious self-interaction of localized states in an effective Hartree-Fock (HF) manner [17]). On this basis, relevant physical mechanisms are clearly singled out with systematic study against various constraints (e.g.: lattice distortion). An interacting effective Hamiltonian can then be “derived” by matching its self-consistent HF mean-field expression with the tight-binding description of LDA+ $U$ . As shown below, this approach not only produces good energies of the systems, but most remarkably also gives wavefunctions with proper degree of mixed symmetry almost identical to the LDA+ $U$  ones.

The results of our systematic study of the electronic structure of  $\text{LaMnO}_3$  are summarized in Fig. 1, in which the total energy gain per unit formula,  $E_{\text{JT}}$ , as a function

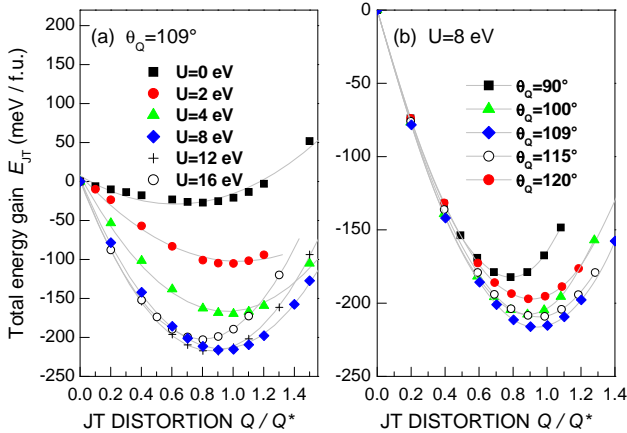


FIG. 1: Total energy gain per formula unit via JT distortion of the  $\text{MnO}_6$  octahedra, expressed in  $\mathbf{Q}_i \equiv (Q_i^z, Q_i^x) = (\sqrt{2}(l-s), \sqrt{2/3}(2m-l-s))$ , with  $l$ ,  $m$ , and  $s$  being the long, medium, and short Mn-O bond lengths, respectively. For long range distortions,  $\mathbf{Q}_i = (Q \cos \theta_Q, e^{i\mathbf{q} \cdot \mathbf{R}_i} Q \sin \theta_Q)$  at the  $i$ -th Mn site located at  $\mathbf{R}_i$ . In low-temperature phases of  $\text{LaMnO}_3$ ,  $Q = Q^* \equiv 0.4 \text{ \AA}$ ,  $\theta_Q = \theta_Q^* \equiv 109^\circ$ , and  $\mathbf{q} = (\pi, \pi, 0)$  [19].

of the JT distortion vector  $\mathbf{Q}_i$  (defined in the caption) is shown for a wide range of the  $U$  parameter of LDA+ $U$  [18, 20]. Notice that for realistic  $U = 8 \text{ eV}$  [18], the crystal structure is stabilized at  $Q^* = 0.4 \text{ \AA}$  [Fig. 1(a)] and  $\theta_Q^* = 109^\circ$  [Fig. 1(b)], in excellent agreement with experiments [19], supporting the good quality of the LDA+ $U$  approximation for this system.

Surprisingly, e-e interaction alone is found *insufficient* to stabilize the orbital ordered insulating phase: for  $U = 0 \text{ eV}$ , the system stabilizes in a metallic state at  $Q = 0.8Q^*$  with small  $E_{\text{JT}} = -27 \text{ meV}$ , despite being weakly insulating at  $Q = Q^*$  with a small gap of 0.1 eV [21]. On the other hand,  $E_{\text{JT}}$  dramatically increases in magnitude to  $-220 \text{ meV}$  as  $U$  increases to 8 eV, indicating that *the electron localization induced by the e-e interaction greatly facilitates the JT instability*—in fact, OO can be stabilized even without JT distortion [17]. Indeed, as shown in Fig. 1(a), fitting the data points to the JT picture ( $E_{\text{JT}} \simeq -\frac{1}{2}gQ + \frac{1}{2}KQ^2$  [12]) is excellent for  $U > 4 \text{ eV}$  but unsatisfactory for small  $U$ , suggesting that only with  $U > 4 \text{ eV}$  the  $e_g$  electrons are well localized as assumed in the JT picture. For realistic  $U = 8 \text{ eV}$ , the JT splitting ( $\sim 4E_{\text{JT}}$  at  $Q^*$ ) is thus  $\Delta_{\text{JT}} \sim 0.9 \text{ eV}$ , comparable to  $\sim 0.8 \text{ eV}$  extrapolated from spectral ellipsometry [8, 9].

For the present study, it is important to carefully distinguish the JT distortion from other lattice distortions, namely octahedral-tilting and its derivative octahedral-distortion of  $\text{GdFeO}_3$ -type. Therefore, our systematic study was performed with the experimental octahedral-tilting angle and crystal volume [20, 22]. Furthermore, octahedral-distortion of  $\text{GdFeO}_3$ -type is found negligible in  $\text{LaMnO}_3$ , as our study of  $\text{LaFeO}_3$ —a JT-inactive coun-

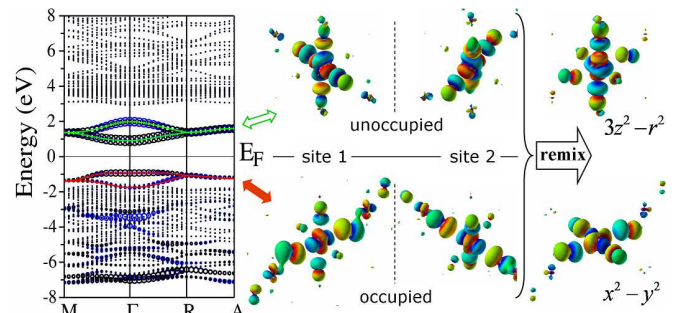


FIG. 2: Left panel: LDA+ $U$  (8 eV) band structure of  $\text{LaMnO}_3$  in the real crystal structure, with circles reflecting the weights of the Mn  $d_{z^2}$  (black) and  $d_{x^2-y^2}$  (blue) symmetries.  $M = (\pi, 0, 0)$ ,  $\Gamma = (0, 0, 0)$ ,  $R = (\pi/2, \pi/2, \pi/2)$ , and  $A = (\pi, 0, \pi/2)$ . Solid green and red lines show the dispersions of OO-relevant spin-majority  $e_g$  Wannier states, illustrated in right panels (see text).

terpart of  $\text{LaMnO}_3$  [23]—produces very small octahedral-distortion with the total energy gain of merely  $-3 \text{ meV}$ . That is, the octahedral-distortions involved in the above calculations are predominantly JT distortions.

In addition to localizing  $e_g$  states, e-e interaction plays other crucial roles, as clearly demonstrated in the LDA+ $U$  (8 eV) band structure (Fig. 2, left panel): The  $\sim 2.6 \text{ eV}$  splitting between the spin-majority occupied and unoccupied  $e_g$  bands near the Fermi energy is too large to be accounted for with the estimated JT splitting ( $\sim 0.9 \text{ eV}$ ), indicating an effective on-site repulsion  $U_{\text{eff}} \simeq 1.7 \text{ eV}$  comparable to the bandwidth. Note that the  $U_{\text{eff}}$  relevant to OO is to be distinguished from the “bare”  $U$  acting between atomic Mn 3d states, as  $U_{\text{eff}}$  acts only between the low-energy  $e_g$  Wannier states (WSs, discussed below), and thus includes effects of additional screening and slight delocalization via hybridization that weaken the “bare” repulsion. Also note that the considerable amount of  $e_g$ -character near the bottom of the oxygen 2p bands ( $[-8, -6] \text{ eV}$ ) is not very relevant to OO, as such feature has its origin in strong hybridization with the oxygen 2p orbitals, independent of ordering of the orbitals. Though it does imply the charge-transfer nature of the manganites in general.

To proceed with more quantitative evaluation of the above effects and to identify other relevant mechanisms, a well-defined local representation of the low-energy  $e_g$  states is necessary for further theoretical formulation. To this end, our previously developed energy-resolved symmetry-specific WF construction [7, 16] is extended to allow mixed symmetry with a constraint search for maximal localization [24]. The resulting orbital ordered occupied ( $[-2.5, 0] \text{ eV}$ ) and unoccupied WSs ( $[0, 2.5] \text{ eV}$ ) are illustrated in Fig. 2 (middle panel), from which the staggered ordering of the orbitals is apparent, as well as the considerable weight at the oxygen sites due to strong  $p$ - $d$  hybridization. Also given in Fig. 2 are the band disper-

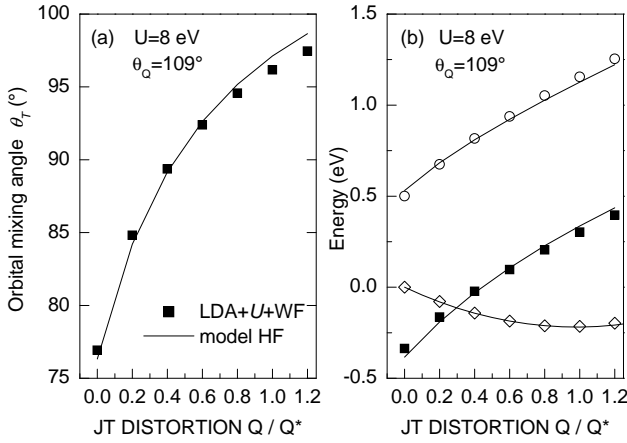


FIG. 3: (a)  $\theta_T$  as a function of JT distortion. (b) Comparison of results from Eq. (3) (lines) and LDA+U+WF:  $H_{i\uparrow,i\uparrow} - H_{i\downarrow,i\downarrow}$  (squares),  $H_{i\uparrow,i\downarrow}$  (circles), and  $E_{\text{JT}}$  (diamonds).  $t = -0.6 \text{ eV}$ ,  $U_{\text{eff}} = 1.72 \text{ eV}$ ,  $gQ^* = 0.87 \text{ eV}$ ,  $K = 2.25 \text{ eV}/\text{\AA}^2$ , and  $E_z = 0.12 \text{ eV}$  are used.

sions (solid lines) corresponding to these WSs, obtained by diagonalizing the tight-binding LDA+ $U$  Hamiltonian,

$$H^{\text{LDA+}U} = \langle jm' | H_{\text{LDA+}U} | jm \rangle, \quad (1)$$

where  $|jm\rangle$  denote the  $m$ -th WS at site  $i$ . For convenient theoretical formulation, a second set of WSs with pure  $d_{3z^2-r^2}$  and  $d_{x^2-y^2}$  symmetries are built from unitary transformation (“remixing”, c.f. Fig. 2) of the first set of WSs. The resulting “conventional” WFs form a realistic basis for our theoretical modeling below.

An important observation emerges from the occupied WSs in Fig. 2: They do not possess the  $d_{3x^2-r^2}$  and  $d_{3y^2-r^2}$  symmetry expected from the JT picture [12]. Indeed, the occupied states  $|occ.\rangle = \cos \frac{\theta_T}{2} |3z^2 - r^2\rangle \pm \sin \frac{\theta_T}{2} |x^2 - y^2\rangle$  do not follow  $\theta_T = \theta_Q = 120^\circ$  from the JT model [12]. As it will become more apparent with the realistic Hamiltonian below, while e-e and e-l interactions induce cooperatively the staggered OO in this system, different mechanisms actually compete in determining the ‘orbital mixing angle’,  $\theta_T$ . Specifically, the purely electronic (superexchange) mechanism [13] favors  $\theta_T = 90^\circ$  for the cubic perovskite structure [25, 26], which was confirmed by our LDA+ $U$  calculations (not shown). This competition makes  $\theta_T$  a *sensitive measure* of the relative importance of leading mechanisms for OO.

An additional relevant mechanism can now be clearly observed from Fig. 3(a), in which  $\theta_T$ , evaluated from the transformation matrix between the above two sets of WFs, is plotted against various magnitude of JT distortion  $Q$  with experimental  $\theta_Q$ . In the absence of the JT effect ( $Q = 0$ ),  $\theta_T = 76^\circ$  is much smaller than  $90^\circ$  expected from the superexchange effect [25, 26]. This reflects the importance of the tetragonal crystal field,  $E_z$ , yielded mainly from the octahedral-titling in the real structure [25], as  $E_z$  favors  $\theta_T = 0^\circ$  instead. Notice also

from Fig. 3(a) that  $\theta_T$  grows as  $Q$  increases, reflecting a sizeable e-l interaction. Nevertheless, even at optimal (experimental)  $\mathbf{Q}$ ,  $\theta_T$  is still way below  $\theta_Q$ , confirming that the JT effect is far from being dominant.

Based on the above systematic analysis of the LDA+ $U$  results, the concrete physics of the low-energy  $e_g$  states can be described by a two-dimensional effective Hamiltonian including  $U_{\text{eff}}$ ,  $\Delta_{\text{JT}}$ , and  $E_z$  [27]:

$$H^{\text{eff}} = \sum_{\langle ij \rangle \gamma\gamma'} t_{ij}^{\gamma\gamma'} d_{j\gamma'}^\dagger d_{i\gamma} + U_{\text{eff}} \sum_i n_{i\uparrow} n_{i\downarrow} - g \sum_i \mathbf{T}_i \cdot \mathbf{Q}_i + \frac{K}{2} \sum_i \mathbf{Q}_i \cdot \mathbf{Q}_i - E_z \sum_i T_i^z, \quad (2)$$

where  $\gamma$  and  $\gamma'$  refer to the second set of WSs, denoting  $|\uparrow\rangle = |3z^2 - r^2\rangle$  and  $|\downarrow\rangle = |y^2 - x^2\rangle$ .  $\mathbf{T}_i = (T_i^z, T_i^x)$  with  $T_i^z = (d_{i\uparrow}^\dagger d_{i\uparrow} - d_{i\downarrow}^\dagger d_{i\downarrow})/2$  and  $T_i^x = (d_{i\uparrow}^\dagger d_{i\downarrow} + d_{i\downarrow}^\dagger d_{i\uparrow})/2$  are pseudo-spin operators. The nearest neighbor anisotropic hopping matrix elements  $t_{ij}^{\gamma\gamma'}$  are  $t_{ij}^{\uparrow\uparrow} = 3t/4$ ,  $t_{ij}^{\downarrow\downarrow} = t/4$ , and  $t_{ij}^{\uparrow\downarrow} = t_{ij}^{\downarrow\uparrow} = \mp\sqrt{3}t/4$ , here the  $\mp$  sign distinguishes hopping along the  $x$  and  $y$  directions.  $g$  is the JT coupling constant and  $K$  is the harmonic elastic constant.

We developed a novel approach to properly map out the model parameters from the LDA+ $U$  results. Employing the fact that strong local e-e interaction is approximated in LDA+ $U$  in an effective HF manner [17], a proper connection can be made on the same WF basis by matching  $H^{\text{LDA+}U}$  with the *self-consistent* HF expression of  $H^{\text{eff}}$ :

$$\sum_{\langle ij \rangle \gamma\gamma'} t_{ij}^{\gamma\gamma'} d_{j\gamma'}^\dagger d_{i\gamma} - \sum_i \mathbf{T}_i \cdot \mathbf{B}_i + \frac{K}{2} \sum_i \mathbf{Q}_i \cdot \mathbf{Q}_i. \quad (3)$$

Here the effective field  $\mathbf{B}_i = (B_i^z, B_i^x)$ , where  $B_i^z = U_{\text{eff}} \langle T_i^z \rangle + (E_z + gQ_i^z)/2$  and  $B_i^x = U_{\text{eff}} \langle T_i^x \rangle + gQ_i^x/2$ .  $\langle T_i^z \rangle = T^z$  and  $\langle T_i^x \rangle = e^{i\mathbf{q} \cdot \mathbf{R}_i} T^x$  with  $\mathbf{q} = (\pi, \pi, 0)$  are the components of the “pseudo-spin density wave” mean field  $\langle \mathbf{T}_i \rangle$ , which must be determined self-consistently and is *not* necessarily parallel to  $\mathbf{Q}_i$ . As shown in Fig. 3, an excellent mapping results from  $t = -0.6 \text{ eV}$ ,  $U_{\text{eff}} = 1.7 \text{ eV}$ ,  $\Delta_{\text{JT}} = gQ^* = 0.9 \text{ eV}$ ,  $K(Q^*)^2/2 = 0.22 \text{ eV}$ , and  $E_z = 0.12 \text{ eV}$ . *Remarkably*, even  $\theta_T = \tan^{-1} T^x/T^z$  obtained from the effective Hamiltonian also agrees well with the LDA+ $U$  results. That is, the effective Hamiltonian accurately reproduce not only all the LDA+ $U$  energies, but also the wavefunctions.

Further insight into the relative importance of e-e and e-l interactions now can be obtained by examining the contribution of each term of the effective Hamiltonian, Eq. (2), to the HF total energy, as shown in Table I. First, consider  $\Delta_0$  (first row), the energy gain purely due to the OO formation (finite  $\langle \mathbf{T}_i \rangle$ ) in the absence of JT distortion. Consistent with the above LDA+ $U$  results, e-e interaction alone ( $-346 \text{ meV}$ ) overwhelms the kinetic energy cost ( $132 \text{ meV}$ ) and induces OO with the total energy gain of  $-223 \text{ meV}$ . More intriguingly, the additional

TABLE I: Contribution of the energy terms in Eq. (2) to  $\Delta_0$  and  $\Delta_{Q^*}$  (see text), in unit of meV per formula unit.

	Total	$U_{\text{eff}}$	$g$	$K$	$E_z$	$t$
$\Delta_0$	-223	-346	0	0	-9	132
$\Delta_{Q^*}$	-220	-257	-356	220	16	158

energy gain via JT distortion  $\mathbf{Q}^*$ , referred to as  $\Delta_{Q^*}$  (second row), consists of considerable further contribution from e-e interaction (-257 meV), without which the JT coupling (-356 meV) alone is insufficient to overcome the energy cost of elastic (220 meV) and additional kinetic (158 meV) energy. That is, e-e interaction, whose contribution is enhanced due to increased  $\langle \mathbf{T}_i \rangle$ , serves as a *hidden driving force* for the octahedral distortion. Overall,  $U_{\text{eff}}$  appears to be more important to OO and the optical gap in  $\text{LaMnO}_3$  than the JT coupling, while their effects on octahedral distortion are comparable.

The present results place stringent constraints on any quantitative theories of the manganites and interpretations of their excitation spectra. For example, there is a current controversy on the recently observed  $120 - 160$  meV Raman shifts of incident photons resonant at  $E_{\text{res}} \simeq 2$  eV [10, 11]. On the one hand, the excitations were interpreted as orbital waves, or ‘orbitons’, derived from the pseudo-spin superexchange model in the large  $U_{\text{eff}}$  limit of Eq. (2) [13]. With the orbiton spectrum gap  $\sim 2.5J_{\text{orb}} + \Delta_{\text{JT}}$  [25, 26, 28] and superexchange coupling constant  $J_{\text{orb}} \simeq 40 - 50$  meV, this scenario requires small  $\Delta_{\text{JT}} \leq 50$  meV [5, 11, 28]. On the other hand, in the JT scenario the Raman shifts were attributed to two-phonon processes (single phonon frequency  $\sim 60 - 80$  meV) induced by a phonon assisted *on-site*  $d_i^4 \rightarrow d_i^4$  transition, requiring large  $\Delta_{\text{JT}} \simeq E_{\text{res}} \simeq 2$  eV [10, 29]. In contrast, our quantitative results ( $\Delta_{\text{JT}} \simeq 0.9$  eV and  $U_{\text{eff}} \simeq 1.7$  eV) show that the spin-majority  $e_g$  states are in the intermediate e-e interaction regime with comparable JT coupling. Therefore, a more reasonable picture would be two-phonon processes mediated by the *inter-site*  $d_i^4 d_j^4 \rightarrow d_i^3 d_j^5$  transition in which  $E_{\text{res}} \simeq 2$  eV [7, 8]. *Direct experimental verification* of our results includes, for example, observation of on-site *d-d* transition ( $\sim 0.9$  eV) via inelastic X-ray scattering or determination of  $\theta_T$  via nuclear magnetic resonance.

In summary, we have quantified the relative importance of e-e and e-l interactions in ordering orbitals in  $\text{LaMnO}_3$  using a new LDA+ $U$ +WF approach. A realistic effective Hamiltonian resulting from this quantitative method reproduces consistently both LDA+ $U$  energies and wavefunctions. Intermediate e-e interaction ( $U_{\text{eff}} \simeq 1.7$  eV) is found to play a crucial role in inducing OO and localizing the electrons, which in turn enhances the JT interaction ( $\Delta_{\text{JT}} \simeq 0.9$  eV) and stabilizes JT distortion. Furthermore, a clear ‘signature’ of competition between e-e and e-l interactions is given via the orbital

mixing angle  $\theta_T < \theta_Q$ . Experimental means to directly clarify the relative strengths of the leading mechanisms are suggested. The developed general theoretical scheme can be applied to other strongly correlated materials.

We are grateful to P. Allen, E. Dagotto, S. Grenier, J. Hill, A.J. Millis, A. Moreo, G. Sawatzky, D. Singh, and J. Thomas for helpful discussions. W.Y. thanks M. Lufaso and P. Woodward for providing SPuDS [23] and T. Chatterji for providing structural data [19]. Brookhaven National Laboratory is supported by U.S. Department of Energy under Contract No. DE-AC02-98CH1-886. This work is partially supported by DOE-CMSN.

---

- [1] E. Dagotto, *Nanoscale Phase Separation and Colossal Magnetoresistance* (Springer Series in Solid State Sciences vol. 136, Springer, 2003).
- [2] T. Hotta, A. L. Malvezzi, and E. Dagotto, Phys. Rev. B **62**, 9432 (2000).
- [3] M. V. Mostovoy and D. I. Khomskii, Phys. Rev. Lett. **92**, 167201 (2004).
- [4] K. H. Ahn and A. J. Millis, Phys. Rev. B **61**, 13545 (2000).
- [5] S. Okamoto, S. Ishihara, and S. Maekawa, Phys. Rev. B **65**, 144403 (2002).
- [6] Y. Murakami, J. P. Hill, D. Gibbs, M. Blume, I. Koyama, M. Tanaka, H. Kawata, T. Arima, Y. Tokura, K. Hirota, et al., Phys. Rev. Lett. **81**, 582 (1998).
- [7] S. Grenier, J. P. Hill, V. Kiryukhin, W. Ku, Y.-J. Kim, K. J. Thomas, S.-W. Cheong, Y. Tokura, Y. Tomioka, D. Casa, et al., Phys. Rev. Lett. **94**, 047203 (2005).
- [8] N. N. Kovaleva, A. V. Boris, C. Bernhard, A. Kulakov, A. Pimenov, A. M. Balbashov, G. Khaliullin, and B. Keimer, Phys. Rev. Lett. **93**, 147204 (2004).
- [9] R. Rauer, M. Rübhausen, and K. Dörr, to be published.
- [10] R. Krüger, B. Schulz, S. Naler, R. Rauer, D. Budelmann, J. Bäckström, K. H. Kim, S.-W. Cheong, V. Perebeinos, and M. Rübhausen, Phys. Rev. Lett. **92**, 097203 (2004).
- [11] E. Saitoh, S. Okamoto, K. T. Takahashi, K. Tobe, K. Yamamoto, T. Kimura, S. Ishihara, S. Maekawa, and Y. Tokura, Nature (London) **410**, 180 (2001).
- [12] J. Kanamori, J. Appl. Phys. **31**, 14S (1960).
- [13] K. Kugel and D. Khomskii, Sov. Phys. JETP **37**, 725 (1973).
- [14] A. J. Millis, Nature (London) **392**, 147 (1998).
- [15] C. M. Varma, Phys. Rev. B **54**, 7328 (1996).
- [16] W. Ku, H. Rosner, W. E. Pickett, and R. T. Scalettar, Phys. Rev. Lett. **89**, 167204 (2002).
- [17] V. I. Anisimov, F. Aryasetiawan, and A. I. Lichtenstein, J. Phys.: Condens. Matter **9**, 767 (1997).
- [18] LDA+ $U$  ( $U=8$  eV,  $J=0.11U$ ) was shown to appropriately describe the  $(\pi, \pi, 0)$  orbital and  $(0, 0, \pi)$  magnetic structures of  $\text{LaMnO}_3$ , see I. S. Elfimov and V. I. Anisimov and G. A. Sawatzky, Phys. Rev. Lett. **82**, 4264 (1999).
- [19] T. Chatterji, F. Fauth, B. Ouladdiaf, P. Mandal, and B. Ghosh, Phys. Rev. B **68**, 052406 (2003).
- [20] All LDA+ $U$  results reported here were obtained with the linear augmented plane wave method [22] for the A-type antiferromagnetic phase with  $J=0.11U$  fixed. Hypothetic crystal structures were prepared with SPuDS [23].

- [21] W. E. Pickett and D. J. Singh, Phys. Rev. B **53**, 1146 (1996).
- [22] P. Blaha *et al.*, Comput. Phys. Commun. **147**, 71 (2002).
- [23] M. W. Lufaso and P. M. Woodward, Acta Cryst. B **60**, 10 (2004).
- [24] W. Ku *et al.*, to be published.
- [25] J. Bala and A. M. Oleś, Phys. Rev. B **62**, R6085 (2000).
- [26] W.-G. Yin, H. Q. Lin, and C. D. Gong, Phys. Rev. Lett. **87**, 047204 (2001).
- [27] In A-type antiferromagnetic  $\text{LaMnO}_3$ , the spin degree of freedom is frozen and hopping along the  $z$  axis is strongly suppressed by the double exchange effect [2, 25, 26].
- [28] J. van den Brink, Phys. Rev. Lett. **87**, 217202 (2001).
- [29] P. B. Allen and V. Perebeinos, Phys. Rev. Lett. **83**, 4828 (1999).